Journal Pre-proof

Synthetic reconstruction of extreme high hydrostatic pressure resistance in *Escherichia coli*

Elisa Gayán, Bram Van den Bergh, Jan Michiels, Chris W. Michiels, Abram Aertsen

PII: S1096-7176(20)30153-1

DOI: https://doi.org/10.1016/j.ymben.2020.09.008

Reference: YMBEN 1726

To appear in: *Metabolic Engineering*

Received Date: 16 July 2020

Revised Date: 18 September 2020

Accepted Date: 21 September 2020

Please cite this article as: Gayán, E., Van den Bergh, B., Michiels, J., Michiels, C.W., Aertsen, A., Synthetic reconstruction of extreme high hydrostatic pressure resistance in *Escherichia coli*, *Metabolic Engineering* (2020), doi: https://doi.org/10.1016/j.ymben.2020.09.008.

Author statement:

E.G. and A.A. designed the experiments. E.G. carried out the experimental work. E.G. and B.V.B analyzed the data. E.G., A.A., B.V.B., J.M. and C.M. wrote, reviewed and edited the manuscript.

Synthetic reconstruction of extreme high hydrostatic pressure resistance in *Escherichia coli*

Elisa Gayán[a#]*, Bram Van den Bergh[ab], Jan Michiels[ab], Chris W. Michiels[a], Abram Aertsen[a]*

[a]Department of Microbial and Molecular Systems, KU Leuven. Faculty of Bioscience Engineering, Kasteelpark Arenberg 20, 3001 Leuven, Belgium.

[b]VIB Center for Microbiology, Flanders Institute for Biotechnology, Kasteelpark Arenberg 20, 3001, Leuven, Belgium.

[#]Current address: Department of Animal Production and Food Science, AgriFood Institute of Aragon (IA2), University of Zaragoza-CITA. Faculty of Veterinary, Miguel Servet 177, 50013 Zaragoza, Spain.

*Address correspondence to Abram Aertsen

abram.aertsen@kuleuven.be

Faculty of Bioscience Engineering

Laboratory of Food Microbiology

Kasteelpark Arenberg 22

B-3001 Leuven

Belgium

Tel: +32 16 32 17 52

Abstract

Although high hydrostatic pressure (HHP) is an interesting parameter to be applied in bioprocessing, its potential is currently limited by the lack of bacterial chassis capable of surviving and maintaining homeostasis under pressure. While several efforts have been made to genetically engineer microorganisms able to grow at sublethal pressures, there is little information for designing backgrounds that survive more extreme pressures. In this investigation, we analysed the genome of an extreme HHP-resistant mutant of *E. coli* MG1655 (designated as DVL1), from which we identified four mutations (in the *cra*, *cyaA*, *aceA* and *rpoD* loci) causally linked to increased HHP resistance. Analysing the functional effect of these mutations we found that the coupled effect of downregulation of cAMP/CRP, Cra and the glyoxylate shunt activity, together with the upregulation of RpoH and RpoS activity, could mechanistically explain the increased HHP resistance of the mutant. Using combinations of three mutations, we could synthetically engineer *E. coli* strains able to comfortably survive pressures of 600-800 MPa, which could serve as genetic backgrounds for HHP-based biotechnological applications.

Keywords: High hydrostatic pressure, engineering of stress resistance, *Escherichia coli*, central carbon metabolism, RpoS activity, heat shock response

1. Introduction

High hydrostatic pressure (HHP) is an important parameter in the biosphere that ranges from atmospheric pressure (0.1 MPa) on the earth's surface to 110 MPa in the deepest part of the ocean (Mariana Trench), and likely even higher pressures in the deep subsurface that might still be colonized with microorganisms (Oger and Jebbar, 2010; Peoples et al., 2019). As described by the thermodynamic principle of Le Châtelier and Braun, HHP can change the organization and function of biomolecules as well as the rate and direction of enzymatic reactions (Eisenmenger and Reyes-De-Corcuera, 2009; Winter and Dzwolak, 2005). Consequently, several industrial applications are emerging or being envisaged from imposing HHP on biological systems (Aertsen et al., 2009; Mota et al., 2013). As such, HHP has been implemented in non-thermal food processing for inactivating undesirable enzymes and microorganisms, while retaining the sensorial qualities of the food (Wang et al., 2016). On the other hand, pressure resistance is a desirable trait in starter or probiotic cultures added in foods that need to fulfil their functions after HHP processing (da Cruz et al., 2010; Speranza, 2020). HHP-mediated modulation of enzymatic reactions and/or substrate availability can also be exploited for accelerating reaction rate, generating new products and/or inhibiting undesirable ones (Eisenmenger and Reyes-De-Corcuera, 2009; Oey, 2016). However, enzymes supporting desired reactions need themselves to be structurally stable and functional under pressure, which could be accomplished by engineering the enzyme or sheltering it in a HHP-resistant cellular environment that would manage to preserve enzyme activity (Huang et al., 2016; Ichiye, 2018). Moreover, there is growing interest in using pressure-tolerant strains for governing rate and direction of biosynthetic pathways in microbial fermentation and bioremediation of deep sea oil spills (Mota et al., 2018; Scoma et al., 2019; Tosi-Costa et al., 2019).

Further exploitation of HHP technology for such biotechnological applications however would require a better understanding of the impact of pressure on bacterial physiology and the corresponding (stress) response and adaptation mechanisms. In fact, this would allow inferring genetic strategies to synthetically engineer HHP compatible or resistant microbial chassis or molecular strategies to preserve enzyme functionality under or after HHP exposure. Such insights can in part be gathered from piezophilic microorganisms that thrive in the deep sea, and that can grow at pressures of up to 130 MPa (Oger and Jebbar, 2010). However, these extremophiles are not adapted to HHP alone, but rather to the deep-sea environment as a whole (Hay et al., 2009; Ichiye, 2018). Together with the lack of genetic tractability (Zhang et al., 2015b), this makes the identification and validation of HHP adaptations more complex. Moreover, strategies for growth tolerance under sublethal HHP conditions do not necessarily coincide with survival mechanisms at higher pressures (Follonier et al., 2012; Gayán et al., 2017b). Another important source of information, however, can stem from mesophiles that, through directed evolution, became forced to very selectively acquire HHP growth tolerance (Marietou et al., 2015) or extreme HHP resistance (Karatzas et al., 2007; Van Boeijen et al., 2011; Vanlint et al., 2012).

In the latter context, *Escherichia coli* seems particularly suited to acquire HHP resistance. In fact, not only is there already quite some variability in HHP resistance among different *E. coli* isolates, directed evolution efforts have also managed to endow this bacterium with extreme HHP resistance (Hauben, 1997; Vanlint et al., 2011; Vanlint et al., 2012). As such, a mutant of *E. coli* K12 MG1655 (designated as DVL1) capable of surviving to pressures in the gigapascal range was isolated after iterative

exposure of the strain to progressively intensifying HHP shocks with intermittent resuscitation and outgrowth (Vanlint et al., 2011). On the contrary, closely related strains, such as *Salmonella enterica*, *Shighella flexneri* and *Yersinia enterocolitica*, appeared less fit to spontaneously acquire HHP resistance under the same selective pressure (Vanlint et al., 2012).

Analysis of HHP-resistant *E. coli* isolates so far indicates that mutants with an upregulated RpoS-mediated stress response are often selected (Vanlint et al., 2013b), which coincides with previous observations on the crucial role of this sigma factor for HHP resistance (Charoenwong et al., 2011; Robey et al., 2001). More recently, acquiring loss-of-function mutations compromising cAMP/CRP regulation has been reported as an alternative evolutionary route towards increased HHP resistance, regardless of basal cellular RpoS activity (Gayán et al., 2017a). Although we have subsequently shown that downregulating cAMP/CRP activity and upregulating RpoS response boosted pressure resistance of *E. coli*, this improvement was still far from the extensive levels of HHP resistance acquired by some spontaneous mutants such as DVL1 (Gayán et al., 2017a).

In this study, we therefore aimed to elucidate the genetic basis of the acquired HHP resistance in DVL1, by first comparing the genome sequences of the evolved mutant and its parental strain and then examining the contribution of identified mutations to the HHP resistance phenotype by synthetically reconstructing each of them and their combinations in the parental background. As a result, *E. coli* chassis with extreme resistance to high pressures (i.e., 600–800 MPa) were engineered with the minimally required genetic changes.

2. Material and methods

2.1. Whole genome sequencing

High-quality genomic DNA of *E. coli* DVL1 (Vanlint et al., 2011) and its MG1655 parental strain (Blattner et al., 1997) was isolated from overnight cultures in Lysogeny Broth (LB) medium (Miller, 1992) incubated aerobically at 37ºC, using the GeneJET Genomic DNA Purification Kit (Thermo Fisher Scientific, Waltham, MA, USA). Paired-end libraries were prepared using the NEBNext Ultra kit and analyzed on the Agilent BioAnalyzer. Sequencing was performed with an Illumina MiSeq sequencer (VIB Nucleomics Core, Belgium), yielding 1,511,848 and 1,823,728 paired-end reads (150 bp) for the WT and DVL1 strain, respectively. CLC Genomics Workbench version 7.5.1 (CLC Bio, Aarhus, Denmark) was used for analysis of the sequences, as previously described by Van den Bergh et al. (2016). Following quality assessment of the raw data, reads were trimmed using quality scores of the individual bases (quality limit = 0.01; maximum number of ambiguous bases = 2). Reads shorter than 15 bases were discarded from the set. Mapping of trimmed reads was performed by the CLC "Map Reads to Reference" algorithm (mismatch cost = 2; insertion cost = 3; deletion cost = 3; length fraction = 0.8; similarity fraction = 0.8) using as a reference the *E. coli* MG1655 genome (NC_000913.2) (Blattner et al., 1997). Mutations were detected using the CLC Fixed Ploidy Variant Detection tool (minimum coverage = 10; minimum frequency = 20%; required significance = 1%) and the InDels and Structural Variants tool (*P*-value threshold = 0.0001; maximum number of mismatches = 3; minimum number of reads = 2). Furthermore, the presence of large deletions or insertions were examined by inspecting coverage distribution and unmapped regions manually.

Mutations found in both WT and DVL1 strains compared to the reference genome were discarded. Finally, the identified mutations were further confirmed with Sanger sequencing analysis, using the primers listed in Table S1.

2.1. Strain and plasmid construction

The *E. coli* strains and plasmids used throughout this investigation are listed in Table S2, while the primers used for constructions are listed in Table S1. LB broth and agar were routinely used for strain and plasmid construction and when necessary, a final concentration of 50 μg/ml of kanamycin (Panreac-AppliChem, Darmstadt, Germany), 20 μg/ml of tetracycline (Sigma-Aldrich, St. Louis, MO, USA), 100 μg/ml of ampicillin (Thermo Fisher Scientific) or 30 μg/ml of chloramphenicol (Sigma-Aldrich) was added to select for the presence of plasmids or recombined amplicons.

The mutations found in DVL1 were identically reconstructed in the parental wild-type (WT) *E. coli* MG1655 by the dual counter-selection system described by Li et al. (2013). Firstly, the homologue region containing the target mutation of DVL1 in the cells of interest, equipped with the plasmid pKD46 (encoding the λ red recombinase genes behind the *araBAD* promoter (Datsenko and Wanner, 2000)), was replaced by an amplicon containing the *tetA-sacB* marker prepared on *E. coli* XTL298. In a second step, counter-selection was used to recombine the *tetA-sacB* cassette with a PCR product obtained on DVL1 using primers flanking the desired mutation. For the point mutation located in the 5' UTR of *rpoD* gene, the *tetA-sacB* cassette was inserted upstream of the point mutation to avoid transcription defects that could affect cell viability (Baba et al., 2006), and the clones lacking the cassette after the counter-selection step were screened for the presence of the mutation by sequencing.

Gene deletions were performed according to the method of Datsenko and Wanner (2000). Briefly, an amplicon prepared on pKD13 (containing the kanamycin resistance cassette [*nptI*]) was recombineered in-frame after the start codon of the target gene of a pKD46 equipped strain. The kanamycin resistance gene was flanked by *frt* sites to be further excised by transiently equipping the strain with the plasmid pCP20 (expressing the Flp site-specific recombinase (Cherepanov and Wackernagel, 1995)). The *rpoD-msfgfp* transcriptional fusions were constructed by obtaining a *msfgfp-frt-nptI-frt* amplicon from the plasmid pDHL1029 (Ke et al., 2016) that was recombineered after the 3' end of *rpoD*. To maximize co-translational activity, the gene encoding *msfgfp* was preceded by a strong synthetic ribosome binding site (BBa_B0034; sequence AAAGAGGAGAA (Elowitz and Leibler, 2000)). The resistance cassette was subsequently excised by transiently equipping the strains with pCP20.

pACYC184-based complementation plasmids were constructed by first amplifying the *cra* and *aceBA* loci of MG1655 (WT) along with their native promoters after primers phosphorylation by T4 polynucleotide kinase (Thermo Fisher Scientific). Please note that *aceA* forms part of the *aceBAK* operon, and since it is located downstream of *aceB* preceded by the operon promoter (Cozzone and El-Mansi, 2005), the *aceAB* transcriptional unit was cloned in the same vector. Then, the obtained products were blunt-ligated (T4 DNA ligase; Thermo Fisher Scientific) to a pACYC184 backbone (Rose, 1988) obtained by PCR amplification, resulting in pACYC184-cra^{WT} (encoding the MG1655 *cra* gene under the control of its native promoter) and pACYC184-$aceBA^{WT}$ (encoding the MG1655 *aceBA* genes under the control of their native

promoter). Where indicated, the strains were transformed with pACYC184-*cra*^{WT}, pACYC184-*aceBA*^{WT} or the corresponding backbone control plasmid (pACYC184 (Rose, 1988)).

All constructed mutants and plasmids were initially confirmed by PCR with primer pairs attaching outside of the region where homologous recombination or ligation occurred (Table S1), and further verified by sequencing (Macrogen, the Netherlands).

2.3. Determination of HHP resistance

The HHP resistance of *E. coli* strains was determined in the stationary phase of growth. Stationary phase cultures were obtained by inoculating 15 ml-test tubes containing 4 ml of Tryptone Soy Broth (TSB; Oxoid, Basingstoke, UK) with a single colony of each strain, which were then incubated aerobically with shaking (300 rpm) for 18 h at 37°C reaching ca. 3×10^9 CFU/ml. When necessary, TSB was supplemented with chloramphenicol to select for the presence of pACYC184-based vectors (Rose, 1988). Cells were harvested by centrifugation (4000 *g*, 5 min) and resuspended in an equal volume of 0.85% KCl (Sigma-Aldrich). A portion of 200 µl of each cell suspension was individually heat sealed in a sterile polyethylene bag after exclusion of the air bubbles and subjected to pressure (500–800 MPa) for 15 min in an 8-ml pressure vessel (HPIU-10000, 95/1994; Resato, Roden, The Netherlands), held at 20 °C with an external water jacket connected to a cryostat. Both the slow pressure increase (100 MPa/min) and the external water jacket attenuated adiabatic heating during pressure build-up. Finally, decompression was almost instantaneous. After treatment, samples were aseptically retrieved from the polyethylene bags and survival was determined as described below.

2.3. Determination of viability and extent of sublethal injury

Samples were serially diluted in 0.85% KCl supplemented with 0.1% bacteriological peptone water (Oxoid), and subsequently 20 µl of each dilution were spread-plated onto Tryptone Soy Agar (TSA; Oxoid) plates. When indicated, cells were also recovered on Violet Red Bile Glucose Agar (VRBGA; Oxoid) as a selective medium to determine the extent of sublethal injury. After 24 h of incubation at 37°C, plates containing between around 20 and 200 colonies were counted, so that the limit of quantification was 1,000 CFU/ml. The logarithmic reduction factor was calculated as log (N_0/N), in which N_0 and N represent the number of survivors in CFU/ml prior and after treatment, respectively. The number of sublethal injured cells was calculated by the difference between the counts on the non-selective (TSA) and the selective medium (VRBGA).

2.4. Evaluation of acetate usage

To examine the ability of acetate usage, we compared the growth on M9 agar (Miller, 1992) supplemented with acetate (1.0%; Acros Organics, Morris Plains, NJ, USA) or D-glucose (0.5%; Sigma-Aldrich) as the sole carbon source. To this end, stationary phase cultures were washed twice and diluted 1/100 in M9 salts, from which a 5-µl drop was spotted on M9-acetate and M9-glucose. After incubation at 37°C for 48 h, growth of each strain on each medium was scored from ++++ (WT growth) to − (no growth).

2.5. Measurement of β-galactosidase activity

The β-glactosidase reporter was used to assess the activity of the RpoD sigma factor (Fischer et al., 1998; Fu et al., 2015), which directs the expression of essential genes for growth at optimal conditions. The assay was carried out as previously described by Miller (1992). Briefly, stationary phase cells were grown in LB supplemented with

1 mM isopropyl β-D-1-thiogalactopyranoside (IPTG; Acros Organics) for 18 h at 37ºC. The β-galactosidase activity of permeabilized cells on ortho-nitrophenyl-β-galactoside (ONPG; Acros Organics) cleavage was measured in a Multiskan RC (Thermo Labsystems, Vantaa, Finland) and expressed in Miller units (MU).

2.6. Measurement of fluorescent gene reporters

Activity of the RpoS sigma factor (directing the expression of the general stress response) was quantified through the activity of the *bolA* promoter (P_{bolA}) using the pFPV-P_{bolA}-*gfp* construct (Gayán et al., 2016), since transcription of *bolA* gene depends on the RpoS sigma factor (Battesti et al., 2011). Activity of the RpoH sigma factor (directing the expression of the heat shock response) was measured through the activity of the *dnaK* promoter (P_{dnaK}) using the pFPV-P_{dnaK}-*gfp* construct (Aertsen et al., 2004), since transcription of the *dnaK* gene depends on RpoH sigma factor (Roncarati and Scarlato, 2017). The fluorescence emitted by these reporters was measured in 200 µl of stationary phase cultures equipped with pFPV-P_{bolA}-*gfp* or pFPV-P_{dnaK}-*gfp* using a Fluoroscan Ascent FL (Thermo 180 Labsystems, Brussels, Belgium). The GFP signal was measured at an excitation wavelength of 480 nm and an emission wavelength of 520 nm. The obtained fluorescence values were divided by the optical density measured at 600 nm (OD_{600}) on the same sample to obtain the relative fluorescence units. Differences in RpoS and RpoH activity were expressed as fold change with respect to the parental strain.

To measure expression of the *rpoD* gene, the *rpoD-msfgfp* transcriptional fusion was chromosomally constructed in the cells of interest, and the signal derived from the reporter was measured by fluorescence microscopy due to its low intensity.

Fluorescence microscopy was performed with a Ti-Eclipse inverted microscope (Nikon, Champigny-sur-Marne, France) equipped with a 60× Plan Apo λ oil objective, a TI-CT-E motorized condenser and a Nikon DS-Qi2 camera. A SpecraX LED illuminator (Lumencor, Beaverton, USA) was used as a light source. GFP was imaged using a triple excitation filter (Ex 473/30) and an emission filter (Em 520/35). For imaging, cells were diluted 1/50 in 0.85% KCl and then placed in 0.85% KCl agarose pads and a cover glass, as previously described (Cenens et al., 2013). Images were taken using the NIS-Elements AR software (Ver. 4.51; Nikon), using identical acquisition parameters for images of the strains to be compared. Image analysis was performed with the open source software MicrobeTracker (Sliusarenko et al., 2011), which estimated average cellular fluorescence of cell meshes generated after background subtraction. The average cellular fluorescence, expressed in arbitrary units (AU), was calculated by dividing the integrated pixel intensities of individual cells by their corresponding areas. A number of ca. 100 cells were evaluated from each independent culture of each strain.

2.7. Statistical analysis

Statistical analyses, ANOVA and *t*-tests, were carried out using the software GraphPad PRISM 5.0 (GraphPad Software Inc., San Diego, CA, USA), and differences were regarded as significant when P was ≤ 0.05. All microbial inactivation outcomes shown in figures correspond to averages and standard deviations calculated from at least three replicates performed in different working days. Miller and fluorescence data correspond to averages and standard deviations obtained from three measurements on independent cultures.

3. Results

3.1 Whole genome sequencing of DVL1

In order to identify the mutations in *E. coli* MG1655 strain DVL1 (further referred to as DVL1) that are potentially linked to its extreme HHP resistance, the whole genome of the evolved mutant and its MG1655 parent was sequenced, yielding on average 53.5 fold and 44.8 fold coverage, respectively. Comparative analysis revealed a total of 5 mutations across the DVL1 genome, which were all confirmed by Sanger sequencing: three single-nucleotide polymorphisms (SNPs), a deletion and an insertion (Table 1).

One of the SNPs was located in the open reading frame (ORF) of the *cra* gene (encoding the catabolism repressor-activator), leading to an amino acid (AA) substitution (Leu56Arg) in the binding domain of the effector metabolite (Vartak et al., 1991). Another was placed in the ORF of the *yhdH* gene (encoding the acrylyl-CoA reductase), resulting in an AA change (Phe77Val) in the catalytic domain (Sulzenbacher et al., 2004). The third SNP was found in the intergenic region between *dnaG* and *rpoD* genes (encoding the DNA primase and RNA polymerase sigma factor D [σ^{70}], respectively), within the 5' untranslated region (UTR) of *rpoD* (Lupski et al., 1984; Yajnik and Godson, 1993). A deletion of 50 bp was found within the ORF of the *aceA* gene (encoding the isocitrate lyase), resulting in a frame-shift from position 1,133 bp and (because of an earlier stop codon) a truncation of the ORF at position 1,179 bp. Finally, an insertion of 5 bp was found within the ORF of the *cyaA* locus, resulting in a frame-shift from position 1,924 bp and (because of an earlier stop codon) a truncation of the ORF at position 1,953 bp, which would remove the regulatory domain of the CyaA protein (Park et al., 2006). This latter mutation was already identified in our previous study (Gayán et al., 2017a).

Position[a]	Gene region	Type of mutation	Nucleotide change	Protein change	Function
88194	ORF of *cra*	SNP	T→G	Leu56Arg	DNA-binding transcriptional dual regulator Cra (catabolite repressor-activator), which controls many genes encoding enzymes involved in carbon metabolism.
3210919	Intergenic region between *dnaG* and *rpoD* (5' UTR of *rpoD*)	SNP	G→A		RNA polymerase sigma factor D (σ^{70}), directing the expression of genes essential for normal growth.
3401734	ORF of *yhdH*	SNP	T→G	Phe77Val	Acrylyl-CoA reductase, involved in acrylate catabolism.
3991098[b]	ORF of *cyaA*	Insertion (5 bp)	Frame-shift resulting in an earlier stop codon	Change from, and including, AA 643 to 650[d] (normal length: 848 AA)	Adenylate cyclase, which synthesizes cAMP for carbon catabolite repression.
4216264-4216313[c]	ORF of *aceA*	Deletion (50 bp)	Frame-shift resulting in an earlier stop codon	Change from, and including, AA 378 to 392[d] (normal length: 434 AA)	Isocitrate lyase, involved in the glyoxylate cycle.

SNP: single nucleotide polymorphism; ORF: open reading frame; 5' UTR: 5' untranslated region; AA: amino acid.

[a]Positions are placed according to the MG1655 reference genome map (NC_000913.2).

[b]The position gives the nucleotide after which the insertion took place.

[c]The positions give, and include, the nucleotides that were deleted.

[d]Total length of the truncated protein.

Table 1. Mutations identified in *E. coli* DVL1.

3.2. Identification of key mutations for increased HHP resistance

We first aimed to identify the key single mutations for increased HHP resistance by individually reconstructing each mutant allele *de novo* in the parental background and comparing their resistance at different pressure levels (Fig. 1). All the single mutations significantly ($P \leq 0.05$) increased HHP survival of the WT strain, except for the SNP found in *yhdH* gene, suggesting that this latter mutation might have trivially hitchhiked along during the selection of DVL1. However, none of the mutations could on its own enforce the level of HHP resistance displayed by DVL1.

The contribution of each mutation to HHP resistance also varied with the applied pressure. The $aceA^{DVL1}$ mutant showed ca. 1 log cycle lower ($P \leq 0.05$) inactivation than the WT strain at 600 MPa and 700 MPa, but no resistance improvement ($P > 0.05$) at 800 MPa. The cra^{DVL1} and $cyaA^{DVL1}$ mutants showed the highest HHP resistance at all pressures, displaying a similar ($P > 0.05$) increase in resistance at low and high pressure (on average 2.3 and 1.9 log cycles at 600 MPa and 800 MPa, respectively) compared to the WT strain. In contrast, the increase in survival of the $rpoD^{DVL1}$ mutant was larger at 700 MPa and 800 MPa (1.7 and 2.0 log cycles, respectively) than at 600 MPa (1.5 log cycles), reaching similar levels ($P > 0.05$) of resistance than the cra^{DVL1} and $cyaA^{DVL1}$ mutants at the highest pressures.

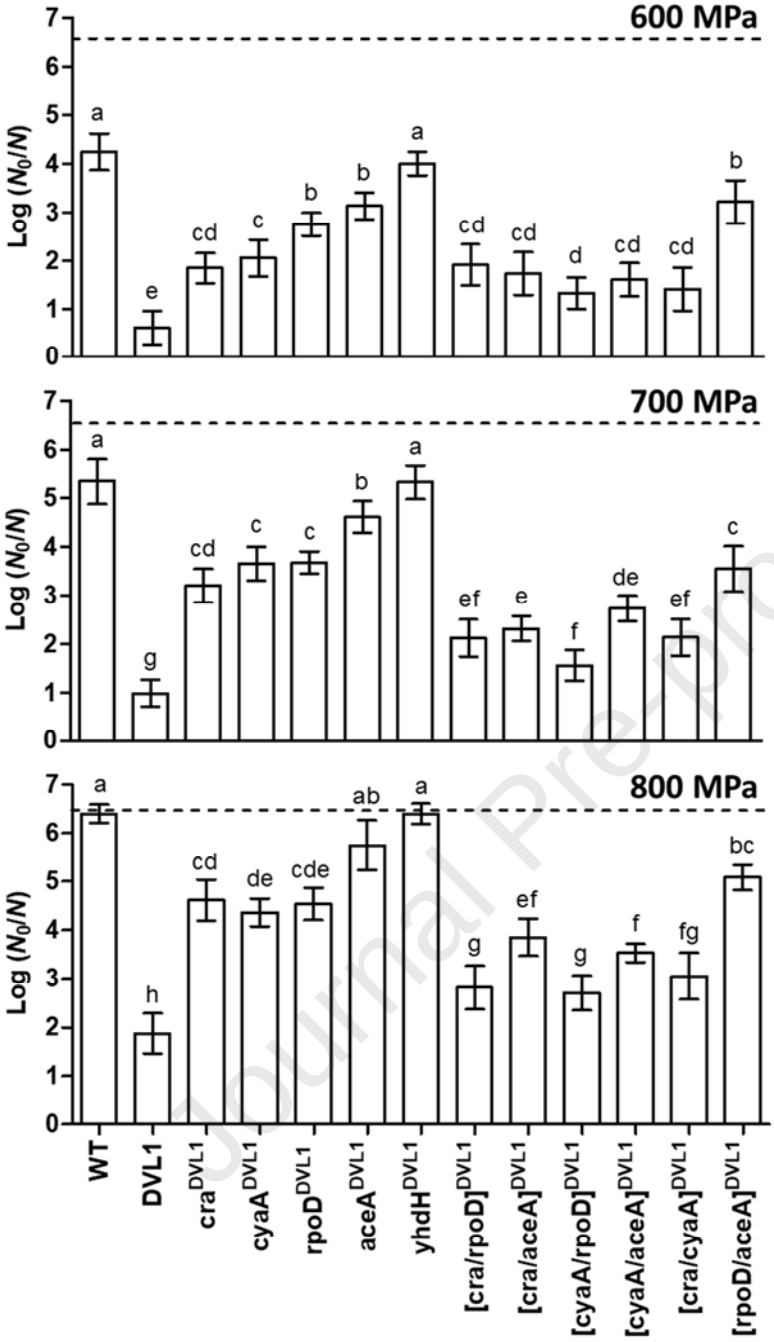

Figure 1. Inactivation (log [N_0/N]) of DVL1, MG1655 (WT) and indicated single and double synthetic mutants of MG1655 by HHP treatment (15 min) at different pressures (600 MPa, 700 MPa and 800 MPa). Survivors were recovered on TSA. The dotted line represents the limit of quantification (1,000 CFU/ml). Letters above each bar allow strains within the same panel to be statistically compared. Strains are only significantly different ($P \leq 0.05$) from each other when they don't share the same letter.

Subsequently, we investigated the effect of synthetically combining two of the key mutations (i.e., *cra*^{DVL1}, *cyaA*^{DVL1}, *rpoD*^{DVL1} and *aceA*^{DVL1}) on MG1655 HHP resistance (Fig. 1). The incorporation of the *aceA*^{DVL1} allele into the *cra*^{DVL1} and *cyaA*^{DVL1} mutants improved ($P \leq 0.05$) their HHP survival by ca. 0.9 log cycles at 700 MPa and 800 MPa, even though at the latter pressure the *aceA*^{DVL1} mutation alone could barely provide HHP protection to the parental strain. However, the strain harbouring the combination of *aceA*^{DVL1} and *rpoD*^{DVL1} mutations showed the same ($P > 0.05$) phenotype than the *rpoD*^{DVL1} mutant at all pressures tested. The combination of the mutations that were most powerful on their own (i.e., [*cra*/*cyaA*]^{DVL1} strain) increased ($P \leq 0.05$) HHP resistance of the single *cra*^{DVL1} and *cyaA*^{DVL1} mutants only at 700 MPa and 800 MPa by ca. 1.3 log cycles. Adding the *rpoD*^{DVL1} mutation to the *cra*^{DVL1} or *cyaA*^{DVL1} strains, however, resulted in a much greater improvement (1.7 log cycles on average at 700 MPa and 800 MPa). The largest effect was observed in the [*cyaA*/*rpoD*]^{DVL1} strain, which showed ca. 3.7 log cycles higher ($P \leq 0.05$) survival than the parental strain at 700 MPa and 800 MPa. Nonetheless, the resistance of the [*cyaA*/*rpoD*]^{DVL1} mutant to all HHP treatments was still much lower ($P \leq 0.05$) than that of DVL1.

We therefore sought to construct strains harbouring triple combinations of mutations (denoted as T_1^{DVL1}, T_2^{DVL1}, T_3^{DVL1} and T_4^{DVL1}; Table S1) that could reproduce the resistance of DVL1 at the highest pressures (Fig. 2). In addition, all the four key mutations were combined in a single strain (denoted as Q^{DVL1}) in order to compare the effect of lacking only one of the alleles in the triple mutants. Moreover, to analyze in even more depth the HHP resistance of the triple and quadruple synthetic mutants in comparison to that of DVL1, survivors were recovered in a non-selective (TSA) and a

selective (VRBGA) medium to determine the extent of sublethal injury. The combination of the most HHP-protective single mutations in the strain T_2^{DVL1} (i.e., [*cra*/*cyaA*/*rpoD*]^{DVL1}) surprisingly resulted in an equal ($P > 0.05$) resistance to that of the [*cra*/*cyaA*]^{DVL1} and [*cra*/*rpoD*]^{DVL1} strains and even lower ($P \leq 0.05$) than that of the [*cyaA*/*rpoD*]^{DVL1} mutant at 700 MPa (Fig. 1 and 2). Furthermore, T_2^{DVL1} proved to be much more sensitive ($P \leq 0.05$) than the three double mutants at 800 MPa. Contrarily, T_1^{DVL1}, T_3^{DVL1} and T_4^{DVL1} mutants (containing [*cra*/*aceA*/*rpoD*]^{DVL1}, [*cra*/*cyaA*/*aceA*]^{DVL1} and [*cyaA*/*aceA*/*rpoD*]^{DVL1} alleles, respectively) finally displayed similar ($P > 0.05$) inactivation than DVL1 at 700 MPa. However, the number of sublethally injured survivors of T_3^{DVL1} was ca. 93% higher ($P \leq 0.05$) than that of DVL1, while T_4^{DVL1} actually incurred 81% lower ($P \leq 0.05$) damaged cells. In fact, the increased HHP resistance of T_4^{DVL1} significantly stood up at 800 MPa, resulting in 37-fold higher ($P \leq 0.05$) survival than DVL1. Interestingly, compared to mutant T_4^{DVL1}, the combination of the four alleles in the quadruple mutant (Q^{DVL1}) showed slightly lower ($P > 0.05$) resistance at 800 MPa and higher extent of sublethal damage at both 700 MPa and 800 MPa.

Overall, the simultaneous presence of three of any of the key mutant alleles could reach similar or even better levels of HHP resistance (at 800 MPa) than DVL1, except for the combination of [*cra*/*cyaA*/*rpoD*]^{DVL1}, which even negatively affected the interaction existing between all its double combinations.

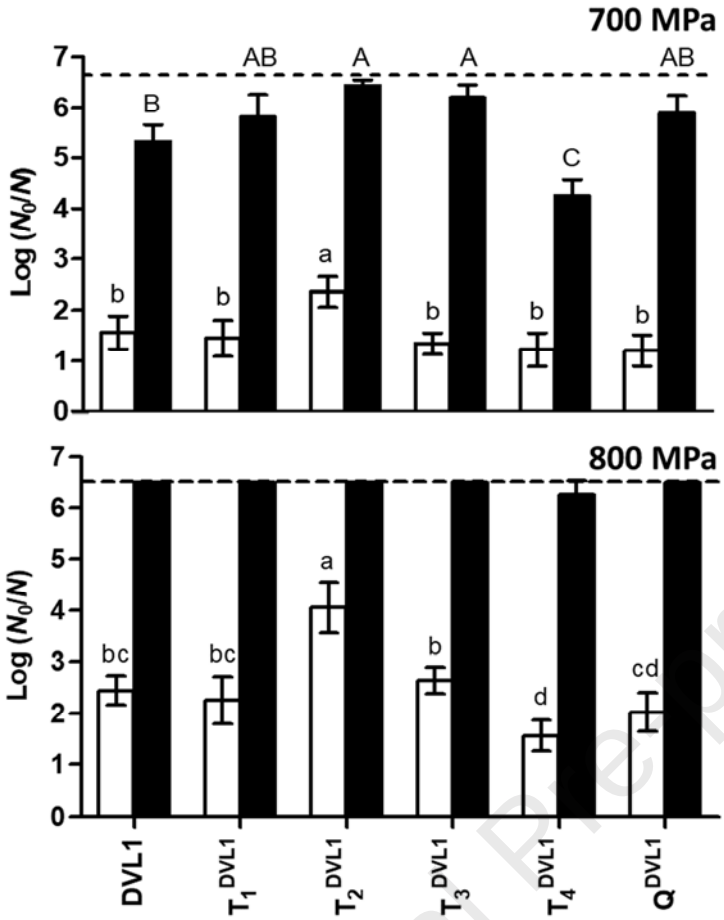

Figure 2. Inactivation (log [N_0/N]) of DVL1 and triple and quadruple synthetic mutants of MG1655 by HHP treatment (15 min) at different pressures (700 MPa and 800 MPa). Survivors were recovered on TSA (white bars) and VRBGA (black bars). The dotted line represents the limit of quantification (1,000 CFU/ml). Letters above each bar allow strains within the same panel and recovery condition to be statistically compared, with lowercase letter referring to recovery on TSA and capital letters referring to recovery on VRBGA. Strains are only significantly different ($P \leq 0.05$) from each other when they don't share the same letter.

3.4. Evaluation of functional effect of key mutations

We then focused on investigating the functional effect of each individual spontaneous mutation that was critical for HHP resistance development in DVL1. To examine the impact of the mutation in the 5' UTR of *rpoD* locus, we measured levels of gene expression in the WT and $rpoD^{DVL1}$ strains harbouring a *rpoD-msfgfp* transcriptional fusion. In addition, RpoD activity was assessed using the β-galactosidase reporter (Fischer et al., 1998; Fu et al., 2015), since expression of the *lacZ* gene (encoding the β-glactosidase enzyme) is mediated by this sigma factor. Although the DVL1 mutation did not affect ($P > 0.05$) *rpoD* promoter activity, it did reduce ($P \leq 0.05$) β-galactosidase activity (Fig. 3A and B), suggesting that the mutant allele could incur an altered somehow posttransciptional regulation that in turn downregulates RpoD activity. Since reduced RpoD levels can affect the competition among sigma factors for the RNA polymerase (Gao et al., 2016; Jishage et al., 2002), we evaluated whether the $rpoD^{DVL1}$-mediated HHP resistance phenotype could stem from alterations in the regulatory function of the RpoS or RpoH sigma factors. In fact, quantifying GFP expression from the *bolA* promoter (using the pFPV-P_{bolA}-*gfp* reporter plasmid (Gayán et al., 2016)) and *dnaK* promoter (using the pPFV-P_{dnaK}-*gfp* reporter plasmid (Aertsen et al., 2004)) as a proxy of basal cellular RpoS and RpoH levels, respectively, showed that attenuated RpoD activity indeed boosted both RpoS- and RpoH-dependent responses (Fig. 4A and B, respectively). Nevertheless, RpoH activity within the DVL1 strain still outperformed (ca. 1.9-fold) that of the $rpoD^{DVL1}$ mutant (Fig. 4B).

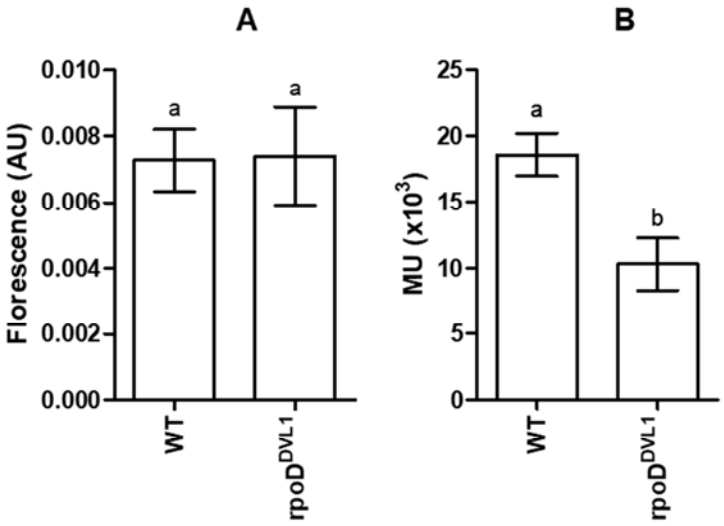

438

439 **Figure 3.** (A) Average cellular fluorescence derived from *rpoD-msfgfp* transcriptional
440 fusion and (B) β-galactosidase activity in MG1655 (WT) and its synthetic *rpoD*^{DVL1}
441 mutant. Letters above each bar allow strains within the same panel to be statistically
442 compared. Strains are only significantly different ($P \leq 0.05$) from each other when they
443 don't share the same letter. AU: arbitrary units. In Fig. A, the number of cells of the WT
444 and *rpoD*^{DVL1} strain evaluated was 281 and 319, respectively.

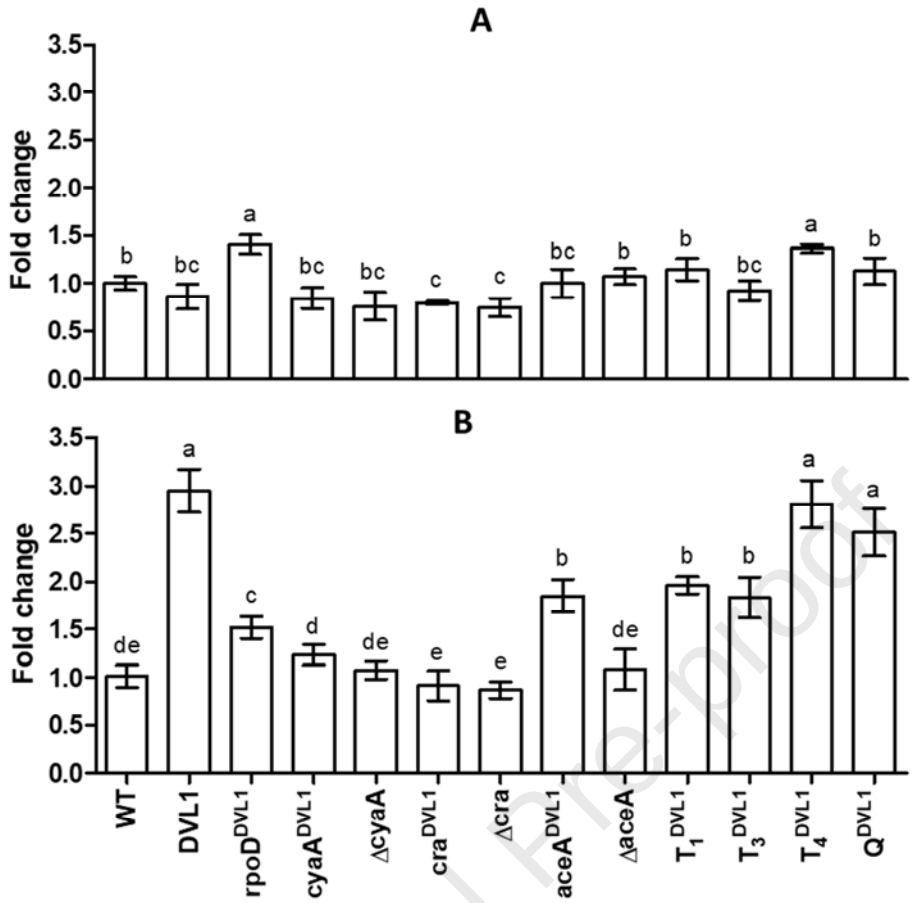

Figure 4. Fluorescence derived from (A) pFPV-P_{bolA}-*gfp* (encoding the *E. coli* MG1655 *bolA* promoter upstream of *gfp*; as a proxy of RpoS activity) and (B) pFPV-P_{dnak}-*gfp* (encoding the *E. coli* MG1655 *dnaK* promoter upstream of *gfp*; as a proxy of RpoH activity) in DVL1, MG1655 (WT) and the indicated synthetic mutants of MG1655. Letters above each bar allow strains to be statistically compared. Strains are only significantly different ($P \leq 0.05$) from each other when they don't share the same letter..

To determine the functionality of cra^{DVL1} and $aceA^{DVL1}$ encoded proteins, we compared the impact of the corresponding wild-type, mutant (i.e., cra^{DVL1} and $aceA^{DVL1}$) and null/deletion alleles (i.e., Δ*cra* and Δ*aceA*) on the ability to grow on glucose (as a control) or acetate as the sole carbon source, since lacking either the catabolite

repressor-activator or the isocitrate lyase impairs the use of acetate (Kim et al., 2018; Maloy and Nunn, 1982). As shown in Table 2, the *cra*^{DVL1} strain, like the Δ*cra* mutant, showed a growth defect on acetate but not on glucose. In agreement, the increased HHP resistance of the Δ*cra* mutant compared to the WT strain at 600 MPa equalled (P > 0.05) that of the *cra*^{DVL1} mutant (Fig. 5). In order to further confirm that compromised Cra activity was causally linked to the *cra*^{DVL1} and Δ*cra* phenotypes, each mutant and the WT strain were equipped with a plasmid-borne copy of the parental *cra* gene (using pACYC184-*cra*^{WT}), and with the pACYC184 vector as a control. The presence of pACYC184-*cra*^{WT} in the *cra*^{DVL1} and Δ*cra* mutants restored their ability to grow on acetate (Table 2) and decreased their HHP resistance to the same levels (P > 0.05) as the WT strain containing the pACYC184-*cra*^{WT} plasmid (Fig. S1A). Measuring P_{bolA} and P_{dnaK} activity, we observed slightly decreased ($P \leq 0.05$) RpoS activity levels in the mutants compared to the WT strain but equal (P > 0.05) RpoH activity levels (Fig. 4). Indeed, the increased RpoS activity derived from *rpoD*^{DVL1} mutation was attenuated in the reconstructed mutants carrying the *cra*^{DVL1} allele (i.e., T_1^{DVL1}, T_3^{DVL1} and Q^{DVL1}), showing the same (P > 0.05) degree of *bolA* activity than the WT strain and DVL1.

Strain	M9-glucose	M9-acetate
WT	++++	++++
WT pACYC184	++++	++++
WT pACYC184-*cra*^{WT}	++++	++++
WT pACYC184-*aceBA*^{WT}	++++	++
Δ*cra*	++++	+
Δ*cra* pACYC184	++++	+
Δ*cra* pACYC184-*cra*^{WT}	++++	++++
cra^{DVL1}	++++	+
cra^{DVL1} pACYC184	++++	+
cra^{DVL1} pACYC184-*cra*^{WT}	++++	++++
Δ*aceA*	++++	-
Δ*aceA* pACYC184	++++	-
Δ*aceA* pACYC184-*aceBA*^{WT}	++++	++
aceA^{DVL1}	++++	-
aceA^{DVL1} pACYC184	++++	-
aceA^{DVL1} pACYC184-*aceBA*^{WT}	++++	++
Δ*cyaA*	++++	-
cyaA^{DVL1}	++++	++

Table 2. Growth of *E. coli* MG1655 (WT) and its derivatives on M9-glucose (0.5%; as a control) and M9-acetate (1.0%) after incubation at 37ºC for 48 h. Growth of each strain on each medium was scored from ++++ (WT growth) to − (no growth).

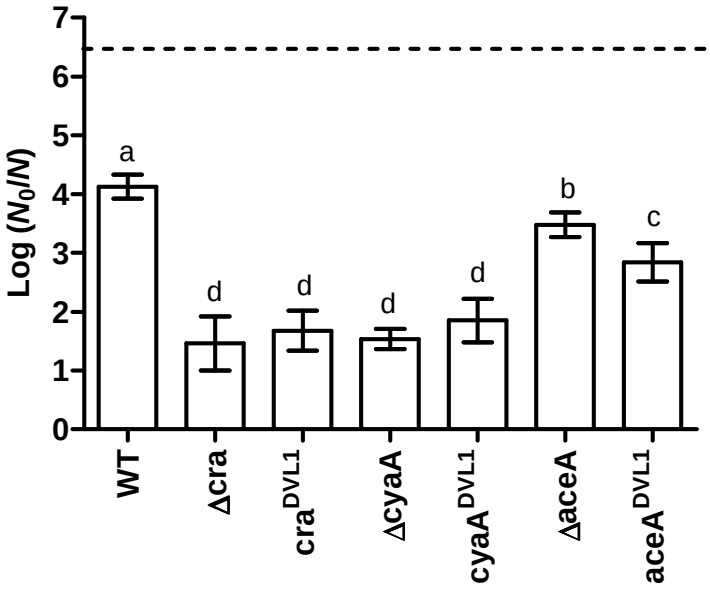

507

508 **Figure 5.** Inactivation (log [N_0/N]) of MG1655 (WT) and indicated synthetic mutants of
509 MG1655 by HHP treatment (15 min) at 600 MPa. Survivors were recovered on TSA.
510 The dotted line represents the limit of quantification (1,000 CFU/ml). Letters above
511 each bar allow strains to be statistically compared. Strains are only significantly
512 different ($P \leq 0.05$) from each other when they don't share the same letter.

513

514

515 Both *aceA*^{DVL1} and Δ*aceA* strains grew poorly on acetate, which agreed with the likely
516 loss-of-function truncation found in the *aceA*^{DVL1} allele. However, the deletion of *aceA*
517 in the WT strain resulted in a 1.0 log cycle higher ($P \leq 0.05$) HHP inactivation (600
518 MPa) than in the strain harbouring the truncated AceA protein (Fig. 5).
519 Complementation of both mutants by a plasmid-borne *aceBA*^{WT} copy (using
520 pACYC184-*aceBA*^{WT}) enabled them to grow on acetate but to a lower degree than the
521 WT strain (Table 2). However, overexpression of *aceBA*^{WT} in the WT strain also
522 impaired the growth on acetate, indicating that *aceBA* overdose attenuated fitness for
523 growth on the secondary carbon source. In concordance, providing the *aceA*^{DVL1} and

524 Δ*aceA* mutants with a native *aceBA*^{WT} copy decreased ($P \leq 0.05$) their HHP sensitivity
525 by ca. 2.9 log cycles, as well as the survival of the WT strain but in a lower extent (2.0
526 log cycles; Fig. S1B). Interestingly, while *aceA*^{DVL1} and Δ*aceA* mutations did not ($P >$
527 0.05) affect levels of P_{bolA} activity (Fig. 4A), the *aceA*^{DVL1} allele caused a 1.9-fold higher
528 ($P \leq 0.05$) P_{dnaK} activity compared to the WT and Δ*aceA* alleles (Fig. 4B). However, the
529 large (ca. 2.9-fold) increase in P_{dnaK} activity as observed in DVL1 was only reached
530 when combining the [*cyaA*/*aceA*/*rpoD*]^{DVL1} alleles in the triple mutant T_4^{DVL1} and, by
531 extension, in the quadruple (Q^{DVL1}) mutant (Fig. 4).
532
533 Regarding the *cyaA* mutation, we previously noted that DVL1 had compromised
534 cAMP/CRP regulation likely due to the loss-of-function mutation incurred in the *cyaA*
535 gene (Gayán et al., 2017a). Consistent to our expectations, synthetic reconstruction of
536 the *cyaA*^{DVL1} allele in the parental MG1655 strain reduced the ability of acetate usage
537 (Table 2) and provided similar levels ($P > 0.05$) of HHP protection (600 MPa; Fig 5)
538 than the complete gene deletion (i.e., Δ*cyaA* strain). As anticipated (Gayán et al., 2017a;
539 Vanlint et al., 2013a), neither *cyaA*^{DVL1} nor Δ*cyaA* mutation increased basal RpoS or
540 RpoH activity of the parental strain (Fig.4).
541
542 Therefore, deletion of *cra*, *aceA* and *cyaA* genes could mimic the phenotypes of the
543 corresponding spontaneous mutant alleles, although the extent of increased HHP
544 resistance provided by the *aceA*^{DVL1} mutation was higher than that of the *aceA* deletion.
545
546 **3.5. Clean synthetic reconstruction of extreme HHP resistance in *E. coli***
547 Finally, we aimed to synthetically reconstruct an extremely HHP resistant *E. coli*
548 chassis in its simplest genetically tangible form. To this end, we created *de novo* the

triple combinations of mutations carried by T_1^{DVL1}, T_3^{DVL1} and T_4^{DVL1} strains (which equalled or surpassed HHP resistance of DVL1; Fig. 2), but completely deleting those genes carrying loss-of-function mutations (i.e., *cra*, *aceA* and *cyaA*) (Fig. 6). Since *rpoD* is an essential gene for cell viability (Baba et al., 2006), the SNP in its 5' UTR had to be identically reproduced for properly compromised RpoD activity. The combination of $rpoD^{DVL1}$ with the *cra* and *aceA* deletions (i.e., T_1^{DVL1} Δ*cra* Δ*aceA* strain) showed ca. 0.7 log cycle lower ($P \leq 0.05$) survival than T_1^{DVL1} at 800 MPa, while incorporating the truncated AceA protein of DVL1 (i.e., T_1^{DVL1} Δ*cra* strain) resulted in similar ($P > 0.05$) survival and sublethal injury levels than DVL1 and T_1^{DVL1} at 700 MPa and 800 MPa. Regarding the combination of *cra*, *cyaA* and *aceA* mutations (i.e., T_3^{DVL1} derivatives), simultaneous deletion of the three genes resulted in ca. 54-fold lower ($P \leq 0.05$) resistance than in T_3^{DVL1} and DVL1 at 800 MPa. Removal of the *cyaA* or *aceA* gene in the T_3^{DVL1} Δ*cra* background led to highly HHP sensitive strains as well, and only the combination of Δ*cra* with the *cyaA* and *aceA* spontaneous mutations reached the same ($P > 0.05$) degree of survival than in T_3^{DVL1}. In agreement, the resistance of strains harboring the $rpoD^{DVL1}$ allele and the deletion of both *cyaA* and *aceA* genes, the deletion of *cyaA* gene with $aceA^{DVL1}$ allele or the deletion of *aceA* gene with $cyaA^{DVL1}$ allele (i.e., T_4^{DVL1} Δ*cyaA* Δ*aceA*, T_4^{DVL1} Δ*cyaA* and T_4^{DVL1} Δ*aceA*, respectively) was markedly lower ($P \leq 0.05$) than T_4^{DVL1}, indicating that the CyaA and AceA truncated proteins provided better fitness for HHP resistance than their absence.

As such, the phenotype of DVL1 could be most cleanly reconstructed by T_1^{DVL1} Δ*cra* (i.e., deleting *cra* and preserving the $rpoD^{DVL1}$ and $aceA^{DVL1}$ alleles) or T_3^{DVL1} Δ*cra* (i.e., deleting *cra* and preserving the $cyaA^{DVL1}$ and $aceA^{DVL1}$ alleles). Nevertheless, when taking sublethal injury into account as well, the T_3^{DVL1} Δ*cra* strain displayed 92%

higher ($P \leq 0.05$) sublethally injured cells than DVL1 after applying the 700 MPa treatment (Fig. 6). The T_4^{DVL1} mutant (containing [*cyaA*/*aceA*/*rpoD*]^{DVL1} alleles), however, remained outperforming all other synthetic reconstructed strains (and even DVL1 itself) in terms of HHP resistance and suppression of sublethal injury.

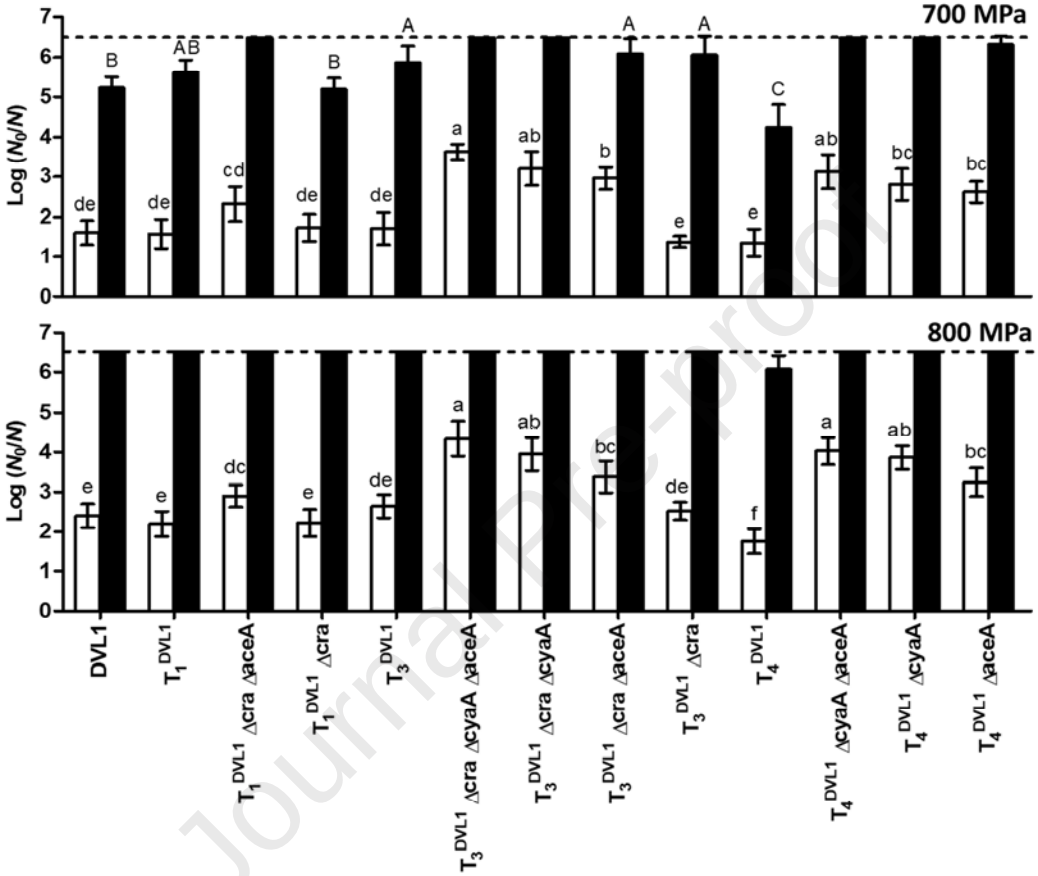

Figure 6. Inactivation (log [N_0/N]) of DVL1, MG1655 (WT) and indicated synthetic mutants of MG1655 by HHP treatment (15 min) at different pressures (700 MPa and 800 MPa). Survivors were recovered on TSA (white bars) and VRBGA (black bars). The dotted line represents the limit of quantification (1,000 CFU/ml). Letters above each bar allow strains within the same panel and recovery condition to be statistically compared, with lowercase letter referring to recovery on TSA and capital letters referring to recovery on VRBGA. Strains are only significantly different ($P \leq 0.05$) from each other when they don't share the same letter.

4. Discussion

Next to metabolic engineering, the building of stress-resistant microbial chassis for applications in bioprocessing under inhospitable conditions or environments is gaining increased attention. As such, the genetic basis for engineering acid-, osmotic-, heat-, and solvent-robust microbial chassis has already been established (Appukuttan et al., 2015; de Siqueira et al., 2020; Jia et al., 2016; Lennen and Herrgård, 2014; Mukhopadhyay, 2015; Swings et al., 2017). However, despite the biotechnological potential of HHP (Aertsen et al., 2009; Speranza, 2020), only little progress has been made on engineering HHP-robust microbial chassis because of the still cryptic multitarget impact of HHP on microbial physiology. In this investigation, we therefore embarked in analyzing the genome of the extremely HHP resistant DVL1 mutant obtained by directed evolution (Vanlint et al., 2011), and used this knowledge to synthetically engineer *E. coli* chassis capable of withstanding pressures of 600-800 MPa.

By comparative genome sequencing and single reconstruction of each mutation found in DVL1, we first identified four key mutations (cra^{DVL1}, $cyaA^{DVL1}$, $aceA^{DVL1}$ and $rpoD^{DVL1}$) causally linked to increased HHP resistance. However, the resistance of DVL1 to the highest pressures could only be reproduced by combining as a minimum three specific mutations, and one of the triple mutants (T_4^{DVL1}, carrying the [*cyaA/aceA/rpoD*]^{DVL1} alleles) even managed to surpass this resistance. On the contrary, the combination of the most HHP-protective individual alleles ([*cra/cyaA/rpoD*]^{DVL1}, carried by T_2^{DVL1}) curiously resulted in antagonistic epistatic interactions, although such effect was alleviated when the four mutations were combined. However, we cannot discard that having disadvantageous combinations of mutations for HHP resistance was

beneficial for the intermediate resuscitation and growth steps imposed on DVL1 during the selection regime (Vanlint et al., 2011).

Analysing the functional effect of each allele, we found that the *rpoD*^{DVL1} mutation, lying in the 5' UTR of *rpoD* (Lupski et al., 1984; Yajnik and Godson, 1993) downtuned RpoD activity, thereby shifting the competition among sigma factors for binding to the RNA polymerase core in favour of RpoS and RpoH activity. Previous investigations have also demonstrated that acquisition of attenuating mutations in the *rpoD* ORF increase activity of stress-related sigma factors and consequently stress tolerance (Gao et al., 2016; Tenaillon et al., 2012; Zhang et al., 2015a). In fact, *rpoD* mutations have been frequently and independently found in mutants obtained by adaptive evolution towards growth tolerance under thermal and acid stress in *E. coli* (Harden et al., 2015; Tenaillon et al., 2012). Accordingly, most of our *E. coli* ATCC 43888 (serovar O157:H7) mutants previously selected for increased HHP or heat resistance displayed upregulated RpoS and/or RpoH activity without their encoding genes and promoters being mutated (Gayán et al., 2016; Vanlint et al., 2013b). Therefore, besides possible mutations that can affect the plethora of factors involved in RpoS and RpoH regulation (Battesti et al., 2011; Roncarati and Scarlato, 2017), changes in RpoD activity and therefore sigma factor balance can be an alternative pathway to acquire HHP resistance. To the best of our knowledge, this is the first described mutation in the 5' UTR of the *rpoD* gene leading to an attenuated RpoD activity. Therefore, from a biotechnological point of view, rewriting this region may be a subtle and appropriate route to synthetically increase stress tolerance without modifying RpoD affinity for certain promoters that could arise from mutations in its ORF (Gao et al., 2016; Tomatis et al.,

637 2019). However, further research is first necessary to decipher the role of the upstream
638 non-coding region of *rpoD* in the regulation of the sigma factor.
639
640 In addition, we corroborated that downregulation of cAMP/CRP activity is one of the
641 most HHP-protective determinants in DVL1. The cAMP/CRP complex controls
642 pleiotropic cellular functions, including non-glucose carbon utilization, central
643 metabolic pathways and stress responses (Gosset et al., 2004; Shimada et al., 2011a),
644 which hampers the identification of components truly involved in HHP resistance.
645 However, it was shown that the HHP resistance provided by the $cyaA^{DVL1}$ allele is not
646 modulated by the RpoS response (Gayán et al., 2017a), and even can complement the
647 increase in resistance provided by upregulating RpoS and RpoH activity. It is
648 noteworthy that complete deletion of the *cyaA* gene impaired the HHP resistance of the
649 strongest strains harbouring the $cyaA^{DVL1}$ allele (i.e., T_3^{DVL1} Δ*cra* vs. T_3^{DVL1} Δ*cra*
650 Δ*cyaA*, and T_4^{DVL1} vs. T_4^{DVL1} Δ*cyaA*), despite the fact that it provided similar levels of
651 resistance than the spontaneous mutant allele in the parental strain. This fact implies
652 that the residual activity of the truncated CyaA or the mere presence of the inactive
653 protein might improve the epistatic interactions among key mutations of DVL1 for HHP
654 resistance.
655
656 Besides cAMP/CRP downregulation, we encountered other mutations affecting central
657 metabolism that are important for HHP resistance. The loss-of-function of Cra provided
658 similar levels of pressure resistance than cAMP/CRP inactivation. Cra represses
659 expression of genes involved in glycolytic pathways by sensing the concentration of
660 fructose-1,6-bisphosphate (FBP) and fructose-1-phosphate (F1P), and activates
661 transcription of genes involved in oxidative and biosynthetic routes, including enzymes

of the tricarboxylic acid (TCA) cycle, electron transfer, glyoxylate shunt and gluconeogenesis (Saier and Ramseier, 1996; Shimada et al., 2011b). In addition, a number of stress response genes are putative targets of the *cra* regulatory network (Shimada et al., 2011b; Son et al., 2011). However, *cra* deletion mutants in *E. coli* have shown increased sensitivity to other stresses such as hyperosmolarity, alcohols and oxidative agents (Egoburo et al., 2018; Son et al., 2011). It is well known that changes in central metabolism impact RpoS activity and by extension stress resistance (Battesti et al., 2015; Gayán et al., 2019). Nonetheless, like in the case of cAMP/CRP downregulation, the role of Cra inactivation in increased HHP resistance was probably not mediated by RpoS and RpoH responses, and even reduced activity of RpoS-dependent promoters. Therefore, the beneficial effects derived from Cra downregulation might predominate over the compromised RpoS activity that it causes.

Despite the extensive overlap between the Cra and cAMP/CRP regulons, identification of common effector genes for increased HHP resistance is still complicated. Firstly, it has been evidenced that Cra positively regulates expression of the *crp* gene (Shimada et al., 2011b; Zhang et al., 2014). However, the fact that combining *cra* and *cyaA* loss-of-function mutations provided higher HHP resistance than the single mutations, rules out that Cra inactivation exerts its effect solely by cAMP/CRP downregulation. Secondly, both transcriptional regulators govern together the expression of several metabolic pathway genes, but generally in opposite directions (Kim et al., 2018; Shimada et al., 2011a; Shimada et al., 2011b). Indeed, it has been demonstrated that the global central metabolism of exponentially growing cells is mainly regulated by Cra and CRP and their regulatory metabolites, and that the dominance among them actually depends on the available carbon substrate for optimal cell growth (Kim et al., 2018; Kochanowski et

al., 2017; Li et al., 2014). Nevertheless, RpoS is also involved in the regulation of central metabolic changes occurring at the entrance of stationary phase (Li et al., 2014; Rahman et al., 2006), and therefore the imbalance among sigma factors mediated by the *rpoD*^{DVL1} allele could also affect possible Cra and cAMP/CRP targets. It should be also considered that other regulators can directly or indirectly participate in the control of many genes shared by the Cra, cAMP/CRP and stress-related sigma regulons. Therefore, a more complex approach encompassing transcriptomic, proteomic and/or metabolomic profiling will be required to trace back effector genes, molecules and metabolic routes involved in the extensive resistance of the reconstructed mutants.

Intriguingly, the *aceBA* genes (encoding the malate synthase and isocitrate lyase acting in the second and first step of the glyoxylate shunt, respectively) are one of the co-regulated loci by Cra and cAMP/CRP. In addition, expression of *aceAB* genes is affected by the interplay between RpoD and RpoS sigma factors (Rahman et al., 2006; Yamamoto and Ishihama, 2003). Regardless of the direction of *aceAB* regulation in the strains carrying mutations downregulating Cra, CyaA and/or RpoD activity, all the best reconstructed HHP-resistant mutants harboured a deleterious mutation in the *aceA* gene shutting down the glyoxylate shunt. The glyoxylate cycle serves to bypass the CO_2-generating steps of the TCA cycle, thus allowing the accumulation of intermediate gluconeogenic substrates and the reduction of NADH levels and the electron flux, which constitute an important defence mechanism against oxidative stress (Rui et al., 2010). However, the truncated AceA of DVL1 provided higher HHP protection than the loss of the complete protein. The presence of the *aceA*^{DVL1} allele, but not the gene deletion, coincided with upregulated heat shock proteins, which has been suggested to play an important role in HHP resistance (Aertsen et al., 2004; Govers et al., 2014).

Therefore, cryptic upregulation of the heat shock response, together with the shutdown of the glyoxylate shunt, might explain the *aceA*^{DVL1} phenotype. However, the increased *dnaK* expression in DVL1 was only reached when combining at least *aceA*^{DVL1}, *rpoD*^{DVL1} and *cyaA*^{DVL1} mutations, even though the latter allele could not change on its own RpoH activity.

In this study, we revealed the genetic basis underlying extreme HHP-resistance in *E. coli*. We also shed light on the physiological mechanisms underlying each key mutation and their interactions in the reconstructed HHP-resistant mutants, signalling the coupled effect of cAMP/CRP downregulation, Cra inactivation, RpoS and RpoH upregulation and/or shutdown of the glyoxylate shunt on their phenotypes. These genetic and physiological insights in *E. coli* HHP-resistance can in the future support the targeted engineering of HHP resistant microbial chassis, and can also serve as a benchmark to understand and predict the broad variations in HHP-resistance that are especially observed among *E. coli* isolates (Liu et al. 205).

Acknowledgements

This work was supported by a postdoctoral fellowship (12P9818N, to E.G.; 12O1917N to B.V.d.B) and a grant (1526416 N) from the Research Foundation - Flanders (FWO-Vlaanderen), and a postdoctoral fellowship (F + /13/040; to E.G.) and a grant (STRT1/10/036) from the KU Leuven Research Fund.

References

Aertsen, A., Vanoirbeek, K., De Spiegeleer, P., Sermon, J., Hauben, K., Farewell, A., Nystrom, T., Michiels, C.W., 2004. Heat shock protein-mediated resistance to high hydrostatic pressure in *Escherichia coli*. Appl. Environ. Microbiol. 70, 2660-2666. https://doi.org/10.1128/aem.70.5.2660-2666.2004.

Aertsen, A., Meersman, F., Hendrickx, M.E.G., Vogel, R.F., Michiels, C.W., 2009. Biotechnology under high pressure: applications and implications. Trends Biotechnol. 27, 434-441. http://dx.doi.org/10.1016/j.tibtech.2009.04.001.

Appukuttan, D., Singh, H., Park, S.-H., Jung, J.-H., Jeong, S., Seo, H.S., Choi, Y.J., Lim, S., 2015. Engineering synthetic multistress tolerance in *Escherichia coli* by using a deinococcal response regulator, DR1558. Appl. Environ. Microbiol. 82, 1154-1166. https://doi.org/10.1128/aem.03371-15.

Baba, T., Ara, T., Hasegawa, M., Takai, Y., Okumura, Y., Baba, M., Datsenko, K.A., Tomita, M., Wanner, B.L., Mori, H., 2006. Construction of *Escherichia coli* K-12 in-frame, single-gene knockout mutants: the Keio collection. Mol. Syst. Biol. 2, 2006.0008-2006.0008. http://dx.doi.org/10.1038/msb4100050.

Battesti, A., Majdalani, N., Gottesman, S., 2011. The RpoS-mediated general stress response in *Escherichia coli*. Annu. Rev. Microbiol. 65, 189-213. https://doi.org/10.1146/annurev-micro-090110-102946.

Battesti, A., Majdalani, N., Gottesman, S., 2015. Stress sigma factor RpoS degradation and translation are sensitive to the state of central metabolism. Proc. Natl. Acad. Sci. U. S. A. 112, 5159-5164. https://doi.org/10.1073/pnas.1504639112.

Blattner, F.R., Plunkett, G., Bloch, C.A., Perna, N.T., Burland, V., Riley, M., Collado-Vides, J., Glasner, J.D., Rode, C.K., Mayhew, G.F., Gregor, J., Davis, N.W., Kirkpatrick, H.A., Goeden, M.A., Rose, D.J., Mau, B., Shao, Y., 1997. The

762 complete genome sequence of *Escherichia coli* K-12. Science. 277, 1453-1462.
763 https://doi.org/10.1126/science.277.5331.1453.
764 Cenens, W., Mebrhatu, M.T., Makumi, A., Ceyssens, P.-J., Lavigne, R., Van Houdt, R.,
765 Taddei, F., Aertsen, A., 2013. Expression of a novel P22 ORFan gene reveals
766 the phage carrier state in *Salmonella* Typhimurium. PLoS Genet. 9.
767 https://doi.org/10.1371/journal.pgen.1003269.
768 Charoenwong, D., Andrews, S., Mackey, B., 2011. Role of *rpoS* in the development of
769 cell envelope resilience and pressure resistance in stationary-phase *Escherichia*
770 *coli*. Appl. Environ. Microbiol. 77, 5220-5229.
771 https://doi.org/10.1128/AEM.00648-11.
772 Cherepanov, P.P., Wackernagel, W., 1995. Gene disruption in *Escherichia coli*: TcR
773 and KmR cassettes with the option of Flp-catalyzed excision of the antibiotic-
774 resistance determinant. Gene. 158, 9-14. https://doi.org/10.1016/0378-
775 1119(95)00193-A.
776 Cozzone, A.J., El-Mansi, M., 2005. Control of isocitrate dehydrogenase catalytic
777 activity by protein phosphorylation in *Escherichia coli*. J. Mol. Microb. Biotech.
778 9, 132-146. https://doi.org/10.1159/000089642.
779 da Cruz, A.G., Fonseca Faria, J.A., Isay Saad, S.M., André Bolini, H.M., Sant′Ana,
780 A.S., Cristianini, M., 2010. High pressure processing and pulsed electric fields:
781 potential use in probiotic dairy foods processing. Trends Food Sci Tech. 21,
782 483-493. https://doi.org/10.1016/j.tifs.2010.07.006.
783 Datsenko, K.A., Wanner, B.L., 2000. One-step inactivation of chromosomal genes in
784 *Escherichia coli* K-12 using PCR products. Proc. Natl. Acad. Sci. U. S. A. 97,
785 6640-6645. https://doi.org/10.1073/pnas.120163297.

de Siqueira, G.M.V., Silva-Rocha, R., Guazzaroni, M.-E., 2020. Turning the screw: engineering extreme pH resistance in *Escherichia coli* through combinatorial synthetic operons. bioRxiv. 2020.02.12.946095. https://doi.org/10.1101/2020.02.12.946095.

Egoburo, D.E., Pena, R.D., Alvarez, D.S., Godoy, M.S., Mezzina, M.P., Pettinari, M.J., 2018. Microbial cell factories a la carte: Elimination of global regulators Cra and ArcA generates metabolic backgrounds suitable for the synthesis of bioproducts in *Escherichia coli*. Appl. Environ. Microbiol. 84, e01337-18. https://doi.org/10.1128/AEM.01337-18.

Eisenmenger, M.J., Reyes-De-Corcuera, J.I., 2009. High pressure enhancement of enzymes: A review. Enzyme Microb. Technol. 45, 331-347. http://dx.doi.org/10.1016/j.enzmictec.2009.08.001.

Elowitz, M.B., Leibler, S., 2000. A synthetic oscillatory network of transcriptional regulators. Nature. 403, 335-338. https://doi.org/10.1038/35002125.

Fischer, D., Teich, A., Neubauer, P., Hengge-Aronis, R., 1998. The general stress sigma factor sigmaS of *Escherichia coli* is induced during diauxic shift from glucose to lactose. J. Bacteriol. 180, 6203-6206.

Follonier, S., Panke, S., Zinn, M., 2012. Pressure to kill or pressure to boost: a review on the various effects and applications of hydrostatic pressure in bacterial biotechnology. Appl. Microbiol. Biotechnol. 93, 1805-1815. https://doi.org/10.1007/s00253-011-3854-6.

Fu, H., Lee, J., Wang, T., 2015. Heat-shock increases RpoD dependent β-galactosidase acctivity in the *Escherichia coli* strains BD792 and B23. J. Exp. Microbiol. Immunol. 19.

Gao, X., Jiang, L., Zhu, L., Xu, Q., Xu, X., Huang, H., 2016. Tailoring of global transcription sigma D factor by random mutagenesis to improve *Escherichia coli* tolerance towards low-pHs. J. Biotechnol. 224, 55-63. https://doi.org/10.1016/j.jbiotec.2016.03.012.

Gayán, E., Cambré, A., Michiels, C.W., Aertsen, A., 2016. Stress-induced evolution of heat resistance and resuscitation speed in *Escherichia coli* O157:H7 ATCC 43888. Appl. Environ. Microbiol. 82, 6656-6663. https://doi.org/10.1128/AEM.02027-16.

Gayán, E., Cambré, A., Michiels, C.W., Aertsen, A., 2017a. RpoS-independent evolution reveals the importance of attenuated cAMP/CRP regulation in high hydrostatic pressure resistance acquisition in *E. coli*. Sci. Reports. 7, 8600. https://doi.org/10.1038/s41598-017-08958-z.

Gayán, E., Govers, S.K., Aertsen, A., 2017b. Impact of high hydrostatic pressure on bacterial proteostasis. Biophys. Chem. 231, 3-9. https://doi.org/10.1016/j.bpc.2017.03.005.

Gayán, E., Rutten, N., Van Impe, J., Michiels, C.W., Aertsen, A., 2019. Identification of novel genes involved in high hydrostatic pressure resistance of *Escherichia coli*. Food Microbiol. 78, 171-178. https://doi.org/10.1016/j.fm.2018.10.007.

Gosset, G., Zhang, Z. G., Nayyar, S. N., Cuevas, W. A., Saier, M. H., 2004. Transcriptome analysis of Crp-dependent catabolite control of gene expression in *Escherichia coli*. J. Bacteriology. 186, 3516-3524. https://doi.org/10.1128/JB.186.11.3516-3524.2004.

Govers, S.K., Dutre, P., Aertsen, A., 2014. In vivo disassembly and reassembly of protein aggregates in *Escherichia coli*. J. Bacteriol. 196, 2325-2332. https://doi.org/10.1128/jb.01549-14.

Harden, M.M., He, A., Creamer, K., Clark, M.W., Hamdallah, I., Martinez, K.A., Kresslein, R.L., Bush, S.P., Slonczewski, J.L., 2015. Acid-adapted strains of *Escherichia coli* K-12 obtained by experimental evolution. Appl. Environ. Microbiol. 81, 1932-1941. https://doi.org/10.1128/AEM.03494-14.

Hauben, K.J., Bartlett, D.H., Soontjens, C.C., Cornelis, K., Wuytack, E.Y., Michiels, C.W., 1997. *Escherichia coli* mutants resistant to inactivation by high hydrostatic pressure. Appl. Environ. Microbiol. 63, 945-950.

Hay, S., Evans, R.M., Levy, C., Loveridge, E.J., Wang, X., Leys, D., Allemann, R.K., Scrutton, N.S., 2009. Are the catalytic properties of enzymes from piezophilic organisms pressure adapted? ChemBioChem. 10, 2348-2353. https://doi.org/10.1002/cbic.200900367.

Huang, Q., Tran, K.N., Rodgers, J.M., Bartlett, D.H., Hemley, R.J., Ichiye, T., 2016. A molecular perspective on the limits of life: Enzymes under pressure. Condens. Matter Phys. 19, 22801. https://doi.org/10.5488/cmp.19.22801.

Ichiye, T., 2018. Enzymes from piezophiles. Semin. Cell Dev. Biol. 84, 138-146. https://doi.org/10.1016/j.semcdb.2018.01.004.

Jia, H., Sun, X., Sun, H., Li, C., Wang, Y., Feng, X., Li, C., 2016. Intelligent microbial heat-regulating engine (IMHeRE) for improved thermo-robustness and efficiency of bioconversion. ACS Synth Biol. 5, 312-320. https://doi.org/10.1021/acssynbio.5b00158.

Jishage, M., Kvint, K., Shingler, V., Nyström, T., 2002. Regulation of sigma factor competition by the alarmone ppGpp. Genes Dev. 16, 1260-1270. https://doi.org/10.1101/gad.227902.

Karatzas, K.A.G., Zervos, A., Tassou, C.C., Mallidis, C.G., Humphrey, T.J., 2007. Piezotolerant small-colony variants with increased thermotolerance, antibiotic

susceptibility, and low invasiveness in a clonal *Staphylococcus aureus* population. Appl. Environ. Microbiol. 73, 1873-1881. https://doi.org/10.1128/AEM.01801-06.

Ke, N., Landgraf, D., Paulsson, J., Berkmen, M., 2016. Visualization of periplasmic and cytoplasmic proteins with a self-labeling protein tag. J. Bacteriol. 198, 1035-1043. https://doi.org/10.1128/jb.00864-15.

Kim, D., Seo, S.W., Gao, Y., Nam, H., Guzman, G.I., Cho, B.-K., Palsson, B.O., 2018. Systems assessment of transcriptional regulation on central carbon metabolism by Cra and CRP. Nucleic Acids Res. 46, 2901-2917. https://doi.org/10.1093/nar/gky069.

Kochanowski, K., Gerosa, L., Brunner, S.F., Christodoulou, D., Nikolaev, Y.V., Sauer, U., 2017. Few regulatory metabolites coordinate expression of central metabolic genes in *Escherichia coli*. Mol. Syst. Biol. 13, 903. https://doi.org/10.15252/msb.20167402.

Lennen, R.M., Herrgård, M.J., 2014. Combinatorial strategies for improving multiple-stress resistance in industrially relevant *Escherichia coli* strains. Appl. Environ. Microbiol. 80, 6223-6242. https://doi.org/10.1128/AEM.01542-14.

Li, X.-t., Thomason, L.C., Sawitzke, J.A., Costantino, N., Court, D.L., 2013. Positive and negative selection using the tetA-sacB cassette: recombineering and P1 transduction in *Escherichia coli*. Nucleic Acids Res. 41, e204-e204. https://doi.org/10.1093/nar/gkt1075.

Li, Z., Nimtz, M., Rinas, U., 2014. The metabolic potential of *Escherichia coli* BL21 in defined and rich medium. Microb. Cell Fact. 13, 45. https://doi.org/10.1186/1475-2859-13-45.

884 Liu, Y., Gill, A., McMullen, L., Gaenzle, M.G. (2015). Variation in heat and pressure
885 resistance of verotoxigenic and nontoxigenic *Escherichia coli*. J. Food Prot. 78,
886 111-120. https://doi.org/10.4315/0362-028x.jfp-14-267.
887 Lupski, J.R., Ruiz, A.A., Godson, G.N., 1984. Promotion, termination, and anti-
888 termination in the rpsU-dnaG-rpoD macromolecular synthesis operon of *E. coli*
889 K-12. Mol. Gen. Genet. 195, 391-401. https://doi.org/10.1007/bf00341439.
890 Maloy, S.R., Nunn, W. D., 1982. Genetic regulation of the glyoxylate shunt in
891 *Escherichia coli* K-12. J. Bacteriology. 149, 173-180.
892 Marietou, A., Nguyen, A.T.T., Allen, E.E., Bartlett, D.H., 2015. Adaptive laboratory
893 evolution of *Escherichia coli* K-12 MG1655 for growth at high hydrostatic
894 pressure. Front. Microbiol. 5, 749. 10.3389/fmicb.2014.00749.
895 Miller, J.H., 1992. A short course in bacterial genetics: A laboratory manual and
896 handbook for *Escherichia coli* and related bacteria. Cold Spring Harbor
897 Laboratory Press, New York. https://doi.org/10.1002/jobm.3620330412.
898 Mota, M. J., Lopes, R. P., Delgadillo, I., Saraiva, J. A., 2013. Microorganisms under
899 high pressure - Adaptation, growth and biotechnological potential. Biotechnol.
900 Adv. 31, 1426-1434. http://dx.doi.org/10.1016/j.biotechadv.2013.06.007.
901 Mota, M.J., Lopes, R.P., Sousa, S., Gomes, A.M., Delgadillo, I., Saraiva, J.A., 2018.
902 *Lactobacillus reuteri* growth and fermentation under high pressure towards the
903 production of 1,3-propanediol. Food Res. Int. 113, 424-432.
904 https://doi.org/10.1016/j.foodres.2018.07.034.
905 Mukhopadhyay, A., 2015. Tolerance engineering in bacteria for the production of
906 advanced biofuels and chemicals. Trends Microbiol. 23, 498-508.
907 https://doi.org/10.1016/j.tim.2015.04.008.

908 Oey, I., 2016. Effects of high pressure on enzymes, in: Balasubramaniam, V.M.,
909 Barbosa-Canovas, G.V., Lelieveld, H.L.M., (Eds.), High Pressure Processing of
910 Food: Principles, Technology and Applications. Springer, New York, pp. 391-
911 431. https://doi.org/10.1007/978-1-4939-3234-4_19.
912 Oger, P.M., Jebbar, M., 2010. The many ways of coping with pressure. Res. Microbiol.
913 161, 799-809. https://doi.org/10.1016/j.resmic.2010.09.017.
914 Park, Y.H., Lee, B.R., Seok, Y.J., 2006. In vitro reconstitution of catabolite repression
915 in *Escherichia coli*. J. Biol. Chem. 281, 6448-6454.
916 https://doi.org/10.1074/jbc.M512672200.
917 Peoples, L.M., Grammatopoulou, E., Pombrol, M., Xu, X., Osuntokun, O., Blanton, J.,
918 Allen, E.E., Nunnally, C.C., Drazen, J. C., Mayor, D.J., Bartlett, D.H., 2019.
919 Microbial community diversity within sediments from two geographically
920 separated hadal trenches. Front. Microbiol. 10, 347-347.
921 https://doi.org/10.3389/fmicb.2019.00347.
922 Rahman, M., Hasan, M.R., Oba, T., Shimizu, K., 2006. Effect of *rpoS* gene knockout on
923 the metabolism of *Escherichia coli* during exponential growth phase and early
924 stationary phase based on gene expressions, enzyme activities and intracellular
925 metabolite concentrations. Biotechnol. Bioeng. 94, 585-595.
926 https://doi.org/10.1002/bit.20858.
927 Robey, M., Benito, A., Hutson, R.H., Pascual, C., Park, S.F., Mackey, B.M., 2001.
928 Variation in resistance to high hydrostatic pressure and *rpoS* heterogeneity in
929 natural isolates of *Escherichia coli* O157:H7. Appl. Environ. Microbiol. 67,
930 4901-4907. https://doi.org/10.1128/aem.67.10.4901-4907.2001.

Roncarati, D., Scarlato, V., 2017. Regulation of heat-shock genes in bacteria: from signal sensing to gene expression output. FEMS Microbiol. Rev. 41, 549-574. https://doi.org/10.1093/femsre/fux015.

Rose, R.E., 1988. The nucleotide sequence of pACYC184. Nucleic Acids Research. 16, 355. https://doi.org/10.1093/nar/16.1.355.

Rui, B., Shen, T., Zhou, H., Liu, J., Chen, J., Pan, X., Liu, H., Wu, J., Zheng, H., Shi, Y., 2010. A systematic investigation of *Escherichia coli* central carbon metabolism in response to superoxide stress. BMC Syst. Biol. 4, 122. https://doi.org/10.1186/1752-0509-4-122

Saier, M.H. Jr., Ramseier, T. M., 1996. The catabolite repressor/activator (Cra) protein of enteric bacteria. J. Bacteriol. 178, 3411-3417. https://doi.org/10.1128/jb.178.12.3411-3417.1996.

Scoma, A., Heyer, R., Rifai, R., Dandyk, C., Marshall, I., Kerckhof, F.-M., Marietou, A., Boshker, H.T.S., Meysman, F.J.R., Malmos, K.G., Vosegaard, T., Vermeir, P., Banat, I.M., Benndorf, D., Boon, N., 2019. Reduced TCA cycle rates at high hydrostatic pressure hinder hydrocarbon degradation and obligate oil degraders in natural, deep-sea microbial communities. ISME J. 13, 1004-1018. https://doi.org/10.1038/s41396-018-0324-5.

Shimada, T., Fujita, N., Yamamoto, K., Ishihama, A., 2011a. Novel roles of cAMP receptor protein (CRP) in regulation of transport and metabolism of carbon sources. PLoS One. 6. https://doi.org/10.1371/journal.pone.0020081.

Shimada, T., Yamamoto, K., Ishihama, A., 2011b. Novel members of the Cra regulon involved in carbon metabolism in *Escherichia coli*. J. Bacteriol. 193, 649-659.

Sliusarenko, O., Heinritz, J., Emonet, T., Jacobs-Wagner, C., 2011. High-throughput, subpixel precision analysis of bacterial morphogenesis and intracellular spatio-

temporal dynamics. Mol. Microbiol. 80, 612-627. https://doi.org/10.1111/j.1365-2958.2011.07579.x.

Son, Y.-J., Phue, J.-N., Trinh, L.B., Lee, S., Shiloach, J., 2011. The role of Cra in regulating acetate excretion and osmotic tolerance in *E. coli* K-12 and *E. coli* B at high density growth. Microb. Cell Fact. 10, 52. https://doi.org/10.1186/1475-2859-10-52.

Speranza, B., Campaniello, D., Petruzzi, L., Altieri, C., Sinigaglia, M., Bevilacqua, A., Corbo, M.R., 2020. The inoculation of probiotics in vivo is a challenge: Strategies to improve their survival, to avoid unpleasant changes, or to enhance their performances in beverages. Beverages. 6, 20. https://doi.org/10.3390/beverages6020020.

Sulzenbacher, G., Roig-Zamboni, V., Pagot, F., Grisel, S., Salomoni, A., Valencia, C., Campanacci, V., Vincentelli, R., Tegoni, M., Eklund, H., Cambillau, C., 2004. Structure of *Escherichia coli* YhdH, a putative quinone oxidoreductase. Acta Crystallogr. D. 60, 1855-1862. https://doi.org/10.1107/s0907444904020220.

Swings, T., Weytjens, B., Schalck, T., Bonte, C., Verstraeten, N., Michiels, J., Marchal, K., 2017. Network-based identification of adaptive pathways in evolved ethanol-tolerant bacterial populations. Mol. Biol. Evol. 34, 2927-2943. https://doi.org/10.1093/molbev/msx228.

Tenaillon, O., Rodríguez-Verdugo, A., Gaut, R.L., McDonald, P., Bennett, A.F., Long, A.D., Gaut, B.S., 2012. The molecular diversity of adaptive convergence. Science. 335, 457. https://doi.org/10.1126/science.1212986.

Tomatis, P. E., Schütz, M., Umudumov, E., Plückthun, A., 2019. Mutations in sigma 70 transcription factor improves expression of functional eukaryotic membrane

proteins in *Escherichia coli*. Sci. Rep. 9, 2483. https://doi.org/10.1038/s41598-019-39492-9.

Tosi-Costa, A.C., Turbay-Vasconcelos, C., Adami, L., Favarato, L., Bolivar-Telleria, M., Carneiro, T., Santos, A., Fernandes, A.R., Fernandes, P.M.B., 2019. High hydrostatic pressure process to improve ethanol production, in: Basso, T.P., Basso, L.C., (Eds.), Fuel Ethanol Production from Sugarcane. IntechOpen, London, pp. 177-197. https://doi.org/10.5772/intechopen.78712.

Van Boeijen, I.K.H., Francke, C., Moezelaar, R., Abee, T., Zwietering, M.H., 2011. Isolation of highly heat-resistant *Listeria monocytogenes* variants by use of a kinetic Modeling-Based Sampling Scheme. Appl. Environ. Microbiol. 77, 2617-2624. https://doi.org/10.1128/aem.02617-10.

Van den Bergh, B., Michiels, J.E., Wenseleers, T., Windels, E.M., Boer, P.V., Kestemont, D., De Meester, L., Verstrepen, K.J., Verstraeten, N., Fauvart, M., Michiels, J., 2016. Frequency of antibiotic application drives rapid evolutionary adaptation of *Escherichia coli* persistence. Nat. Microbiol. 1, 16020. https://doi.org/10.1038/nmicrobiol.2016.20.

Vanlint, D., Mitchell, R., Bailey, E., Meersman, F., McMillan, P.F., Michiels, C.W., Aertsen, A., 2011. Rapid acquisition of Gigapascal-high-pressure resistance by *Escherichia coli*. mBio. 2, e00130. https://doi.org/10.1128/mBio.00130-10.

Vanlint, D., Pype, B.J.Y., Rutten, N., Vanoirbeek, K.G.A., Michiels, C.W., Aertsen, A., 2013a. Loss of cAMP/CRP regulation confers extreme high hydrostatic pressure resistance in *Escherichia coli* O157:H7. Int. J. Food Microbiol. 166, 65-71. http://dx.doi.org/10.1016/j.ijfoodmicro.2013.06.020.

Vanlint, D., Rutten, N., Govers, S.K., Michiels, C.W., Aertsen, A., 2013b. Exposure to high hydrostatic pressure rapidly selects for increased RpoS activity and general

stress-resistance in *Escherichia coli* O157:H7. Int. J. Food Microbiol. 163, 28-33. http://dx.doi.org/10.1016/j.ijfoodmicro.2013.02.001.

Vanlint, D., Rutten, N., Michiels, C.W., Aertsen, A., 2012. Emergence and stability of high-pressure resistance in different food-borne pathogens. Appl. Environ. Microbiol. 78, 3234-3241. https://doi.org/10.1128/aem.00030-12.

Vartak, N.B., Reizer, J., Reizer, A., Gripp, J.T., Groisman, E.A., Wu, L.F., Tomich, J. M., Saier, M.H., 1991. Sequence and evolution of the FruR protein of *Salmonella typhimurium*: a pleiotropic transcriptional regulatory protein possessing both activator and repressor functions which is homologous to the periplasmic ribose-binding protein. Res. Microbiol. 142, 951-963. https://doi.org/10.1016/0923-2508(91)90005-U.

Wang, C.-Y., Huang, H.-W., Hsu, C.-P., Yang, B.B., 2016. Recent advances in food processing using high hydrostatic pressure technology. Crit. Rev. Food Sci. Nutr. 56, 527-540. https://doi.org/10.1080/10408398.2012.745479.

Winter, R., Dzwolak, W., 2005. Exploring the temperature–pressure configurational landscape of biomolecules: from lipid membranes to proteins. Phil. Trans. Math. Phys. Eng. Sci. 15, 537-563. https://doi.org/10.1098/rsta.2004.1507.

Yajnik, V., Godson, G.N., 1993. Selective decay of *Escherichia coli dnaG* messenger RNA is initiated by RNase E. J. Biol. Chem. 268, 13253-13260.

Yamamoto, K., Ishihama, A., 2003. Two different modes of transcription repression of the *Escherichia coli* acetate operon by IclR. Mol. Microbiol. 47, 183-194. https://doi.org/10.1046/j.1365-2958.2003.03287.x.

Zhang, F., Qian, X., Si, H., Xu, G., Han, R., Ni, Y., 2015a. Significantly improved solvent tolerance of *Escherichia coli* by global transcription machinery

engineering. Microb. Cell Fact. 14, 175-175. https://doi.org/10.1186/s12934-015-0368-4.

Zhang, Y., Li, X., Bartlett, D. H., Xiao, X., 2015b. Current developments in marine microbiology: high-pressure biotechnology and the genetic engineering of piezophiles. Curr. Opin. Biotech. 33, 157-164. https://doi.org/10.1016/j.copbio.2015.02.013.

Zhang, Z., Aboulwafa, M., Saier, M. H., 2014. Regulation of *crp* gene expression by the catabolite repressor/activator, Cra, in *Escherichia coli*. J. Mol. Microb. Biotech. 24, 135-141. https://doi.org/10.1159/000362722.

Highlights

- The genome of an extreme HHP-resistant *E. coli* mutant and its parent were analyzed.
- Four identified mutations were causally linked to increased HHP resistance.
- HHP-resistant strains were engineered by combining some of the three mutations.
- Decreased cAMP/CRP, Cra, and/or AceA activity, and increased RpoH and/or RpoS activity, explained the increased HHP resistance in the mutants.